Hourly and Daily Urban Water Demand Predictions Using a Long Short-Term Memory Based Model

Mu, Li; Zheng, Feifei; Tao, Ruoling; Zhang, Qingzhou; Kapelan, Zoran

DOI
10.1061/(ASCE)WR.1943-5452.0001276

Publication date
2020

Document Version
Accepted author manuscript

Published in
Journal of Water Resources Planning and Management

Citation (APA)
Mu, L., Zheng, F., Tao, R., Zhang, Q., & Kapelan, Z. (2020). Hourly and Daily Urban Water Demand Predictions Using a Long Short-Term Memory Based Model. *Journal of Water Resources Planning and Management*, *146*(9), Article 05020017. https://doi.org/10.1061/(ASCE)WR.1943-5452.0001276

Hourly and daily urban water demand predictions using a long short-term memory based model

Li Mu, Feifei Zheng*, Ruoling Tao, Qingzhou Zhang and Zoran Kapelan

Li Mu: Deputy Chief Engineer, Hefei Water Supply Group Co., Ltd, muli@hfwater.cn

Feifei Zheng: Corresponding author, Professor, College of Civil Engineering and Architecture, Zhejiang University, 866 Yuhangtang Rd, Hangzhou, China 310058. feifeizheng@zju.edu.cn

Ruoling Tao: Master Student, College of Civil Engineering and Architecture, Zhejiang University, taoruoling@zju.edu.cn

Qingzhou Zhang: Postdoctoral fellow, College of Civil Engineering and Architecture, Zhejiang University, 866 Yuhangtang Rd, Hangzhou, China 310058. wdswater@gmail.com

Zoran Kapelan, Professor, Delft University of Technology, Faculty of Civil Engineering and Geosciences, Department of Water Management, Stevinweg 1, 2628 CN Delft, Netherlands. z.kapelan@tudelft.nl

Abstract:

This case study uses a long short-term memory (LSTM) based model to predict short-term urban water demands for the Hefei City of China. The performance of the LSTM based model is compared with autoregressive integrated moving average (ARIMA) model, the support vector regression (SVR) model and the random forests (RF) model based on data with time resolutions ranging from 15-minute to 24-hour. Additionally, this paper investigates the performance of the LSTM based model in predicting multiple successive data points. Results show that the LSTM based model can offer predictions with improved accuracy than the other models when dealing with data with high time resolutions, data points with abrupt changes and data of a relatively high uncertainty level. It is also observed that the LSTM based model exhibit the best performance in predicting multiple successive water demands with high time resolutions. In addition, the inclusion of external parameters (e.g., temperature) cannot enhance the performance of the LSTM based model, but it can improve ARIMAX's prediction ability (ARIMAX is the ARIMA with variables). These obtained insights based on the Hefei case study provide additional and improved knowledge as well as evaluations regarding the LSTM based models used

for short-term urban water demand forecasting, thereby enabling their wider take-ups in practical applications.

Key words: Water demand prediction; long short-term memory; data-driven models; ARIMA models

Introduction

Urban water demand predictions are often important to the sustainable management of water supply systems for a range of purposes, including system design, maintenance and operation (Billings and Jones, 2008; Zheng et al. 2016, 2017; Qi et al., 2018). Accurate urban demand forecasts have become even more vital for many cities in recent years due to the emerged water crisis as a result of rapid urbanization and climate change, as well as driven by the need of real-time system operation (Hutton and Kapelan, 2014; Pacchin et al., 2019). This, consequently, has motived intensive studies to develop models for urban demand prediction, thereby enabling an effective water usage planning and scheduling (Pacchin et al., 2019).

A number of models are available for urban water demand forecasts with different prediction periodicity and forecast horizon (Donkor et al., 2014). More specifically, long-term forecasts usually focus on time periods more than ten years, often providing guidance for city planning and development (Levin et al., 2006). Medium-term forecasts often predict demands at a monthly or yearly resolution, and these predictions are mainly used to develop strategies for water usages (Ghiassi et al.,

55 2008). Short-term forecasts at hourly or daily resolutions are generally employed to
56 enable the effective operations of water treatment plants or pumping stations,
57 typically aimed to provide sufficient demands for urban users with the lowest
58 operation cost (Guo et al., 2018).

59 Traditionally, urban demand forecast models are generally developed based on
60 statistical methods (Howe and Linaweaver, 1967). This is because demand variations
61 are often driven by a group of factors including meteorological parameters and
62 socioeconomic elements (Arbués et al., 2003). Therefore, various linear regression
63 models are used to reveal the underlying relationships between urban water demands
64 and the external affecting parameters, thereby providing long-term demand forecasts
65 based on the projections of the external parameters (e.g., populations, Jain et al.,
66 2001). However, the accuracies of these simple linear regression models are often
67 unsatisfactory, especially in the case of predicting short-term urban water demands
68 (e.g., daily, Wong et al., 2010).

69 In recognizing the potential limitation of simple linear regression models, many
70 data-driven models have been developed to improve demand forecast accuracy

71 (Donkor et al., 2014). Autoregressive models, one type of data-driven models, have
72 been widely used in both the academic field and engineering community, in which a
73 time series analysis is often used to analyze the historical data (Chen and Boccelli,
74 2018). It has been widely demonstrated that these autoregressive models, such as
75 autoregressive integrated moving average (ARIMA) model, can exhibit better
76 performance than traditional linear regression models in predicting short-term urban
77 water demands (Chen and Boccelli, 2018).

78 In parallel to the development of the autoregression models, many other
79 data-driven models are also proposed to predict urban water demands
80 (Ghalehkhondabi et al., 2017). These include artificial neural networks (ANNs) that
81 have been broadly used for urban water demand forecasts (Ghiassi et al., 2008), the
82 support vector regression (SVR, Bai et al., 2015) model and the random forests (RF,
83 Chen et al., 2017) model that also show great merits for demand predictions. These
84 advanced data-driven models have shown improved performance than many
85 traditional prediction methods, such as autoregressive models (Villarin and
86 Rodriguez-Galiano, 2019).

In recent years, a type of recurrent neural networks named as the long short-term memory (LSTM) based model has been emerged as an important prediction tool (Guo et al., 2018). Compared to traditional ANNs, the LSTM based model is better suited for time-series predictions as they possess the ability to preserve previous information through learning time series data, thereby improving the accuracy of predictions (Mikolov et al., 2010, Zhang et al., 2018). While the LSTM based models have been broadly used in the area of artificial intelligence, such as language processing (Sundermeyer et al., 2012), speech recognition (Graves and Jaitly, 2014), and image captioning (Wang et al., 2016). To our best knowledge, only limited studies have been undertaken so far to apply the LSTM based models to predict short-term urban water demands. Guo et al. (2018) have made the first attempt to implement the LSTM method for urban water demand predictions. In the study of Guo et al. (2018), the performance of the LSTM based model has been compared with ARIMA and ANNs based on data with 15-minute resolution, and results showed that the LTSM based models exhibited better capacity than the other two methods in predicting accurate water demands.

Given that the LSTM has only been investigated in Guo et al. (2018), there is therefore a lack of sufficient case study application experience as well as comprehensive understanding on its performance in dealing with short-term urban water demand forecasts. These include how the LSTM based models perform (i) when handling urban water demand predictions with various time resolutions as only 15-minute resolution data were considered in Guo et al. (2018), (ii) when predicting inflection data points that have abrupt changes relative to their corresponding nerbouring demand values, as well as data with a relatively high uncertainty level, (iii) when comparing with other advanced data-driven models such as SVR and RF models, in addition to the traditional ARIMA model considered in Guo et al. (2018), and (iv) when predicting data with a 24-hour time resolution with the aid of external covariates (such as temperature and rainfall). The present case study paper aims to provide additional and improved knowledge as well as evaluations regarding the LSTM' performance in predicting short-term urban water demands, thereby enabling the wider up-takes of the LSTM based models for real-world applications.

Short-term urban water demand prediction models

As previously stated, the ARIMA, SVR and RF models are selected to enable the performance comparison with the LSTM based models. The ARIMA is chosen due to its wide applications in both the academic and industry fields, representing a standard urban water demand prediction model (Guo et al., 2018). The SVR and RF models are selected because they are advanced data-driven models that have shown great merits for urban water demand forecasts (Bai et al., 2015, Chen et al., 2017), and hence it is interested to demonstrate whether the LSTM based model (also a type of data-driven model) can outperform the SVR and RF models or not (this comparison has not been done in the area of the urban water demand prediction).

The long short-term memory (LSTM) based model

A recurrent neural network (RNN) model is a specific kind of artificial neural networks (ANNs), where the network of a RNN typically has connections between neurons and form a directed cycle (Sutskever et al., 2014). This type of structure creates an internal self-looped cell, which allows dynamic temporal behavior. The gradients of RNNs can be computed via Backpropagation Through Time (BPTT)

algorithm (Gers et al., 2000), but this method is inefficient when learning patterns from long-term dependency. To solve this problem, a long-short term memory (LSTM) has been developed, where it is featured by that it can bring information crossing several time steps, and hence prevent early signals from fading away (Zhang et al., 2018). The main structure of the LSTM network is illustrated in Figure 1 (Gers, 2001), stressing the importance of three gates within the algorithm structure. These are input gate, forget gate and output gate, with each gate represented by a sigmoid neural network layer (σ) and a multiplicative unit ($\times$). These components allow the weights converge dynamically, even though the model parameters are fixed.

The LSTM network computes a mapping from an input sequence to an output sequence by calculating network unit activations using the equations as follows (Gers et al., 2000):

$$i_t = \sigma(W_i x_t + U_i h_{t-1} + b_i) \quad (1)$$

$$f_t = \sigma(W_f x_t + U_f h_{t-1} + b_f) \quad (2)$$

$$o_t = \sigma(W_o x_t + U_o h_{t-1} + b_o) \quad (3)$$

$$g_t = \tanh(W_g x_t + U_g h_{t-1} + b_g) \quad (4)$$

$$s_t = g_t \otimes i_t + s_{t-1} \otimes f_t \quad (5)$$

$$h_t = \tanh(s_t) \otimes o_t \quad (6)$$

where $\otimes$ denotes element-wise multiplication of two vectors; t denotes the current time; W_i, W_f, W_o, W_g, U_i, U_f, U_o and U_g denote the weights; b_i, b_f, b_o and b_g denotes the bias; σ and $\tanh$ are the sigmoid functions; x_t is the input vector; i_t refers to the input threshold; f_t is the forget threshold; o_t refers to the output threshold; g_t is the candidate cell state generated by the tanh neural network layer; s_t is the cell state at time t; h_t is the output vector. Specifically, the forget gate controls whether the cell state of previous time is forgotten or not (Equation 2) and the input gate is responsible for the input series at the current time (Equations 1). The two gates act on the updating of current cell state (Equation 5) and then generate the output with the output gate (Equations 3 and 6). One output h_t is the input of the recurrent procedure as shown in Figure 1. Consequently, the LSTM method can prevent the gradient explosion or vanishing issues during error back flow, and predict the output with updated index.

Autoregressive integrated moving average (ARIMA)

The development of ARIMA model can be dated back to 1976 by Box and Jenkins (1976), and this model describes data sequence using linear functions of previous data and random errors. The ARIMA is featured by its great ability to capture the trend, seasonality and randomness of time series (Williams, 2001). Generally, an ARIMA model consists of an autoregressive (AR) model, a difference process that deals with non-stationary data, and a moving average (MA) model, with details presented in Hao et al., (2013).

Support vector regression (SVR) models

The core concept of the support vector regression (SVR) model is that it uses a relatively small number of support vectors to represent the entire sample set and then figures out a curve that can minimize the residual error for the data (Rasouli et al., 2011). Given a set of l samples $[(x_1, y_1), \ldots, (x_l, y_l)]$, where x_i are the input vectors and y_i are the corresponding output values (i=1, 2, …, l), a group of functions $f(x, \alpha)$ can be formulated to approximate the relationship between the x_i and y_i, where α is the

parameter vector of the function. Generally, a nonlinear decision function of an SVR model ($f(w, b)$) can be expressed as:

$$f(w,b) = w \cdot \phi(x) + b \tag{7}$$

where w and b are the parameter vectors of the function; x is the input vector; $\phi(x)$ is a nonlinear function. The objective of the SVR model is to select a function from the group of $f(x, \alpha)$ that can predict the output value as accurately as possible, which is obtained by the minimization of the empirical risk R_{emp} as shown below,

$$R_{emp} = \frac{1}{N}\sum_{i=1}^{N} L_{\varepsilon}\big(y - f(x)\big) \tag{8}$$

where L_{ε} is the loss function between the observations (y) and model predictions ($f(x)$), with details given in Gunn (1998). To solve the objective function in Equation (8), a standard quadratic programming algorithm with a dual set of Lagrange multipliers is often adopted (Yu et al., 2006), which is

$$\min_{w,b,\xi,\xi^*} \frac{1}{2}\sum_{i,j=1}^{l}(\alpha_i - \alpha_i^*)\big(\alpha_j - \alpha_j^*\big)\langle x_i \cdot x_j\rangle + \varepsilon\sum_{i=1}^{l}(\alpha_i + \alpha_i^*) - \sum_{i=1}^{l} y_i(\alpha_i - \alpha_i^*) \tag{9}$$

with constraints

$$\sum_{i=1}^{l}(\alpha_i - \alpha_i^*) = 0 \tag{10}$$

$$0 \leq \alpha_i, \alpha_i^* \leq C, i=1, 2, \ldots, l \tag{11}$$

where C is the error penalty factor; l is the length of the training data; $\langle x_i \cdot x_j \rangle$ is the inner product of x_i, x_j; α_i and α_i^* are the Lagrange multipliers for the i^{th} data point; ε is the error tolerance which is specified by the users (ε=0.1 is often used). To deal with nonlinear regressions, $\langle x_i \cdot x_j \rangle$ in Equation (9) is replaced by the computation of $\langle \phi(x_i) \cdot \phi(x_j) \rangle$ often using a radial basis function (RBF, Yu et al., 2006) as shown below,

$$\langle \phi(x_i) \cdot \phi(x_j) \rangle = e^{-\gamma |x_i - x_j|^2} \tag{12}$$

where γ is a user-defined parameter. In this study, the value of C and γ are determined based on a grid search method as described in Cherkassky and Ma (2004).

Random forests (RF)

Given an input vector X and the corresponding output Y, the random forests (RF) model builds a number of q regression trees formed as $\hat{h}(X, S_n^{\theta_q})$ followed by averaging the results, which can be presented as (Villarin and Rodriguez, 2019)

$$Y = \frac{1}{\mathrm{q}} \sum_{l=1}^{q} \hat{h}(X, S_n^{\theta_l}) \tag{13}$$

Where S_n is the training set; n is the number of observations; the bagging method selects several bootstrap samples $(S_n^{\theta_1}, \ldots, S_n^{\theta_q})$, and accordingly a set of trees

201 $(\hat{h}(X, S_n^{\theta_1}), \ldots, \hat{h}(X, S_n^{\theta_q}))$; θ is the independent identically distributed random

202 variables representing the random selection.

203 Generally, two parameters need to be pre-specified for a RF model, that is, the

204 number of decision trees to be generated (q) and the number of selected input

205 variables m_t for each split θ. Since a RF model is often computationally efficient and

206 does not overfit, q can be set to a relatively large value (Guan et al., 2013). The

207 selection of m_t is based on the following equation (Were et al., 2015),

$$m_t = \left[\sqrt{m}\right] \tag{14}$$

208 where m is the total number of input variables (covariates), [x] denotes the ceiling

209 function of x.

210 ***Benchmarking metrics***

211 Four metrics are considered in this study to enable the statistical analysis of the

212 model performance. These are the mean absolute percentage error (*MAPE*), the

213 Nash-Sutcliffe model efficiency (*NSE*), the coefficient of determination (R^2) and the

214 root mean square error (*RMSE*). Lower values of *MAPE* and *RMSE* indicate better fits

215 of the models, and larger values of *NSE* (the best value is 1) and R^2 (the best value is

1) represent better model performance These four metrics are selected due to their wide applications in the area of urban water demand forecasts (Chen et al., 2017, Zhang et al., 2018). The *MAPE* is defined as

$$MAPE = \frac{1}{N}\sum_{i=1}^{N}\left|\frac{Y_i - \hat{Y}_i}{Y_i}\right| \times 100\% \quad (15)$$

where Y_i represents the i^{th} observed value, and $\hat{Y}_i$ is the i^{th} prediction value; N is the total number of data points being predicted; $\left|\frac{Y_i - \hat{Y}_i}{Y_i}\right|$ is the absolute relative error.

The NSE is defined as

$$NSE = 1 - \frac{\sum_{i=1}^{n}\left(Y_i - \hat{Y}_i\right)^2}{\sum_{i=1}^{n}(Y_i - \bar{Y})^2} \quad (16)$$

where $\bar{Y}$ is the mean of the observations. The R^2 is defined as

$$R^2 = \frac{\left(\sum_{i=1}^{n}\left(Y_i - \tilde{Y}\right)(Y_i - \bar{Y})\right)^2}{\sum_{i=1}^{n}\left(Y_i - \tilde{Y}\right)^2 \sum_{i=1}^{n}(Y_i - \bar{Y})^2} \quad (17)$$

where $\tilde{Y}$ is the mean of the predictions. The *RMSE* is defined as

$$RMSE = \sqrt{\frac{\sum_{i=1}^{n}(Y_i - \hat{Y}_i)}{n}} \quad (18)$$

Case study

Case study description

The LSTM based model has been validated and its performance has been

compared to other three models on water demand records with a 15-minute resolution in the city of Hefei, China. This city has a population of approximately eight million, and the total water demands were approximately 0.59 billion m^3 per year. As shown in Figure 2, a total of seven water treatment plants (WTPs) are used to supply water to this city. Such a large number of WTPs induces high operational complexities for this system, and hence short-term water demand forecasts are important to enable an effective operation of this system, thereby saving the clean water production and operational cost. More specifically, the demand predictions of the 15-min resolution can greatly facilitate the real-time modelling of this water supply system, which can be accordingly used to, for example, enable the leakage and energy analysis (Creaco et al. 2017). The 1-hour demand predictions are often utilized to determine optimal scheduling strategies for the pump stations in the WTPs, thereby reducing the operation cost (Guo et al. 2018).

A total of 70,080 records at a 15-min resolution from May 2016 to May 2018 have been collected from the local water utility in the city of Hefei. These demand records are the total readings from the outflow meters at the water treatment plants as

243 there are no tanks in this water supply system. Figure 3(a) shows one-week records
244 with 15-min resolution for the total demands (TD), and Figure 3(b) presents one-week
245 demands with 15-minute resolution for a district metering area (DMA) within this
246 water supply system. It is seen that the demands of this DMA are very small relative
247 to the total demands of the entire city (TD), implying that this DMA only provides
248 water for a very small population size. Consequently, the demands of this DMA are
249 significantly more variable than the total demands as visualized in Figure 3,
250 representing a dataset with a relatively high uncertainty level.

251 ***Computational experiments and model parameterizations***

252 A number of R and Python packages were used to develop the prediction models
253 applied to the case study. More specifically, the LSTM models were developed in the
254 python environment, with the aid of the functions from Keras library (Chollet, 2015).
255 R packages of "TSA", "e1071" and "randomForest" were used to develop the
256 ARIMA, SVM and RF models respectively (Chang and Lin, 2001; Breiman, 2001).
257 The inputs of the LSTM based models were determined based on a comprehensive
258 sensitivity analysis, following the method outlined in Guo et al. (2018). More

specifically, for the LSTM based model applied to data with 15-min and 1-hour resolutions, the timeline of the inputs was divided into three fragments, the current day, the previous day and the day before yesterday. In each time fragment, a certain number of data points between zero and ten have been tried to identify the inputs that have the best performance. For the LSTM based model applied to data with 24-hour resolution, one to ten previous consecutive days were tried as the inputs. The selected inputs with the best model performance were presented in Table 1. As shown in this table, to predict the data with the 15-min resolution at time *t* of the current day (Q_t^0), the inputs were the demands of previous three time steps at the current day (Q_{t-3}^0, Q_{t-2}^0, Q_{t-1}^0), demands of five consecutive time steps centered at time *t* at the previous day ($Q_{t-2}^{-1}, Q_{t-1}^{-1}, Q_t^{-1}, Q_{t+1}^{-1}, Q_{t+2}^{-1}$), and demands of five consecutive time steps centered at time *t* at the day before yesterday ($Q_{t-2}^{-2}, Q_{t-1}^{-2}, Q_t^{-2}, Q_{t+1}^{-2}, Q_{t+2}^{-2}$). In a similar way, the inputs of the 1-hour and 24-hour resolutions for the LSTM based models, as well as the inputs for the SVR and RF models were outlined in Table 1. For the ARIMA model with 15-minute and 1-hour resolution at time *t*, the inputs were their corresponding previous 672 consecutive data points as presented in Table 1, and the

275 previous 56 consecutive data points with 24-hour resolution were used to predict the
276 24-hour demand at time *t*.

277 A sensitivity analysis was conducted to determine the appropriate architecture
278 for the LSTM model, and the number of layers was 2 with the number of nodes being
279 128 and 16 respectively, the learning rate was 0.002, tanh and ReLU were used as the
280 activation functions, the number of epochs was 100 and the batch size was 60 (Guo et
281 al., 2018). The ARIMA parameters were automatically determined after model
282 calibrations. For the SVR models, the range of the C parameters was integer numbers
283 between 1 and 10, and potential γ values were 0.05, 0.06, 0.07, 0.08, 0.09, 0.1, 0.15
284 and 0.20 following the approach outlined in Friedrich and Igel (2005). Finally, C=1
285 and γ=0.06 were selected using the grid search method as this parameter combination
286 exhibited the best model performance (Cherkassky and Ma, 2004). For the RF models,
287 the number of decision trees q=1000 and m_t=4 based on the method described in Guan
288 et al. (2013). It is noted that the ARIMA models needed to be re-calibrated for each
289 new set of inputs, while RNNs, SVR and RF models only calibrated once using the
290 training data set. The training dataset were records of the first 21 months and data of

291 the last three months were used for model validations.

292 **Results and Discussions**

293 ***Performance comparisons of models applied to total water demands***

294 Figure 4 presents the predictions versus the observations for the four models
295 applied to the total water demands (TD) with different time resolutions. All the four
296 models were able to capture the overall trend of the observations, with errors mainly
297 produced at the extreme values of the observations. The detailed comparisons of these
298 four models are given below.

299 Boxplots in Figure 5 show the absolute relative errors of the predictions
300 generated by the four models applied to the total water demands (TD). It is noted that
301 these results were produced using the validation dataset. It is seen that the LSTM
302 based model exhibited moderately better performance than the other three models for
303 data with 15-minute and 1-hour resolutions, while the four models performed overall
304 similarly when dealing data with the 24-hour resolution. The LSTM's better
305 performance relative to its counterparts can also be supported by the statistics of the
306 prediction errors in Table 2. As shown in this table, the *MAPE* value of the LSTM

307 based models for the 15-minute and 1-hour resolution data were 1.40% and 2.56%
308 respectively, which were lower than those provided by other models. For all different
309 time resolutions, the values of *NSE* and R^2 of the LSTM based models were
310 consistently higher than the other models as shown in Table 2. For the *RMSE* values,
311 the LSTM based model also showed better performance than the other three models
312 for 15-min and 1-hour time resolutions, but it performed similarly with the ARIMA
313 for the 24-hour resolution as shown in Table 2. It is noted that the extreme values of
314 the absolute relative errors are not presented in Figure 5 for the sake of easy
315 comparisons of the overall results.

316 ***Model comparisons for predicting multiple successive data points***

317 It is practically meaningful to predict multiple successive high time resolution
318 data as these predictions can be used to facilitate the decision-making regarding the
319 operation strategies for water production and pumping. Following the method used in
320 Guo et al. (2018), the prediction at time *t* was used as the potential inputs to predict
321 water demands at time *t*+1, thereby predicting multiple successive data points (the
322 number is referred as *k*). For instance, *k*=4 indicated that four successive data points

were generated using the model, and the *MAPE*, *NSE,* R^2 and *RMSE* values were computed based on successive data predictions relative to their corresponding observations.

In this study, the data with the 15-minute resolution were employed for model developments, aimed to predict k=4 (1-hour time period) and 96 (24-hour time period) successive data points, with results given in Figure 6. It is seen that while all models exhibited deteriorated prediction accuracy as the number of k increased, the LSTM based model performed significantly better than the ARIMA, SVR and RF models, with advantages being more noticeable for a larger value of k. For instance, the *MAPE* values of the LSTM based model were 2.21% and 5.23% for k=4 and k=94 respectively as shown in Table 3, which were appreciably lower than the other three models. Similar observations can be made for the *NSE*, R^2 and *RMSE* values as outlined in Table 3.

It is observed from Figure 6 and Table 3 that the performance of the ARIMA model deteriorated in a significantly quicker rate compared to the other three models when the value of k increased. This can be also supported by the results shown in

Figure 7, where large deviations were observed for the ARIMA predictions relative to the observations, especially for k=96. The performance variation between the LSTM based models (also the SVR and RF models) and the ARIMA model in predicting multiple successive data points was caused by the differences of their model structures. More specifically, the inputs of the LSTM based models (also SVR and RF models) were formed by some records in the current day and some data points taken from previous days (see Table 1), while the inputs of the ARIMA model were many successive records before the prediction time. This, consequently, leads to that a larger number of inputs of the ARIMA model would be replaced by the forecasts compared to the LSTM based models, SVR and RF models when predicting multiple successive data points ahead, resulting in larger accumulative errors within the predictions.

Model comparisons for data points with abrupt changes

The data points with abrupt changes are often difficult to predict, and hence they can be used to demonstrate the ability of the prediction models. In this study, a new

dataset was extracted from the original observations using the following procedures. Firstly, each data point was compared with its first previous data point and first data point behind in terms of relative errors, followed by the identification of inflection points based on the signs of the relative errors. Secondly, these inflection data points were ranked based on their mean of the absolute relative errors in a descending order, and finally a new dataset was formed by the first 10% of the ranked data points. Within practical applications, these data points were often referred as “abrupt points”, which were of great interest as many models often failed to produce accurate predictions for them. In this study, the dataset with abrupt changes was respectively extracted from the original 15-minute and 1-hour observations to enable the prediction analysis, as shown in Table 4.

Interestingly, the LSTM based model exhibited significantly better performance than the other three models when applied to datasets with abrupt changes as shown in Table 4. This was supported by that the *MAPE* values of the LSTM based models were lower than 3% for both datasets with 15-minute and 1-hour time resolutions, while *MAPE* values of the other models were all around 5%. We also compared the

371 *MAPE* values of the four models used to produce multiple successive data points for
372 the dataset with abrupt changes extracted from 15-minute observations, with results
373 given in Table 4. Clearly, the LSTM based models also appreciably outperformed the
374 ARIMA, SVR and RF models, with similar observations when measured using *NSE*,
375 R^2 and *RMSE* metrics. Combining the results (Table 2 and 3) that the four models
376 applied to the full dataset, it can be deduced that the advantage of the LSTM based
377 models relative to the other three models can be more prominent when applying to
378 data with abrupt changes.

379 ***Model comparisons for data with a relatively high uncertainty level***

380 Table 5 shows the validation results measured by four statistic metrics of the four
381 models applied to the DMA demands with different time resolutions. As shown in this
382 table, the overall performances of the four models for this DMA demands were worse
383 than those from the total demands of the water supply system (see Table 2), especially
384 for the 15-min and 1-hour resolutions. This was expected as the DMA demands were
385 quite small relative to the total demands of this supply system and hence its demand
386 uncertainty was higher, resulting in challenges for the prediction models.

387 It is seen from Table 5, the LSTM based models consistently outperformed the
388 ARIMA, SVR and RF models for the dataset from the DMA demands. For instance,
389 for the LSTM applied to this dataset with 15-min resolution, *MAPE*=11.77%,
390 *NSE*=0.924, R^2=0.935, and *RMSE*=0.74 m^3 were achieved, which were better than
391 those from the other three models. Same observations can be made for the four
392 models applied to DMA demands with 1-hour and 24-hour time resolutions.

393 ***Model comparisons when accounting for external parameters***

394 To examine the influence of external parameters on the models' performance, a
395 range of parameters were considered as the covariates to develop the models for the
396 total water demands with the 24-hour resolution. These include daily maximum
397 temperature (T_{max}), the daily average of the temperature (T_{avg}), and the accumulative
398 daily rainfall (R_c) as these external parameters have been demonstrated to be
399 important influential factors that could affect the prediction accuracy of the models
400 (Bai et al., 2015).

401 Figure 8 presents the results of the four models with external parameters
402 considered as covariates for model calibrations and validations, where *NC* indicated

403 that no external parameter were used. It was observed that external parameters had
404 limited impacts on the performances of the LSTM based models, but they can slightly
405 enhance the prediction accuracy of the ARIMA, SVR and RF models, especially
406 when the daily maximum temperature (T_{max}) was used as the covariate. Similar
407 observations can be made based on *MAPE*, *NSE*, R^2 and *RMSE* metric values.

408 **Conclusions**

409 This case study paper proposed the use of the long short-term memory (LSTM)
410 network for short-term urban water demand predictions, motivated by that the LSTM
411 networks have already been demonstrated to be an effective forecast tool in many
412 other research fields. To systematically demonstrate the performance of the LSTM
413 based models, the autoregressive integrated moving average (ARIMA) model that has
414 been widely used so far, as well as the support vector regression (SVR) model and the
415 random forest (RF) model that have shown great potentials for urban demand
416 predictions were also implemented in this study. These four models were applied to
417 urban demand predictions with different time resolutions ranging from 15-minute to
418 24-hour for the Hefei City of China. The main observations based on the case study

419 results obtained are as follows,

420 (i) The LSTM based models exhibited better performance than the ARIMA,
421 SVR and RF models in predicting data with high time resolutions (e.g., 15-minute and
422 1-hour), with merits being more significant when handling data points with abrupt
423 changes and data with a relatively high uncertainty level. When predicting data with
424 relatively low time resolutions (e.g., 24-hour), the four models performed overall
425 similarly in terms of prediction accuracy. These observations are practically
426 meaningful as they can be used to facilitate the selection of the appropriate models for
427 real-world problems based on the data properties. In addition, it was found that the
428 LSTM based model showed the significantly improved performance when predicting
429 multiple successive high time-resolution demands, with advantage being more
430 noticeable for the larger number of successive data points. Such ability is of great
431 importance as it is often very important to predict a series of successive demands with
432 a high time resolution, thereby enabling the optimal decision regarding real-time
433 operation strategies.

434 (ii) External parameters such as temperature and rainfall had limited impacts on

435 the performance of the LSTM based models in predicting data with 24-hour
436 resolution, indicating that the performance of the LSTM based model was dominated
437 by its great ability in capturing the underlying relationships within the data
438 themselves. This is also a great merit of the LSTM based models for practical
439 applications as collecting external parameters in a high time resolution is often
440 time-consuming and costly.

441 The observations mentioned above based on the Hefei Case study provide
442 important additional experiences and evaluations regarding the applications of the
443 LSTM based models for short-term urban demand forecasts. These knowledge go
444 beyond the findings reported in Guo et al (2018) as in their study only data with
445 15-min resolution were considered (no covariates), as well as that the LSTM based
446 models were only compared with ARIMA and ANN models. In addition, this study
447 demonstrated that the LSTM based models can exhibit significantly better
448 performance than other models in predicting data points with abrupt changes as well
449 as data with a high uncertainty level, which have not been considered in Guo et al.
450 (2018).

Data Availability Statement

All data, models, or code generated or used during the study are available from the corresponding author by request (feifeizheng@zju.edu.cn).

Acknowledgments

This work is funded by the National Natural Science Foundation of China (Grant No. 51922096), Excellent Youth Natural Science Foundation of Zhejiang Province in China (LR19E080003), Funds for International Cooperation and Exchange of the National Natural Science Foundation of China (No.51761145022), and National Science and Technology Major Project for Water Pollution Control and Treatment (2017ZX07201004).

References

Adamowski, J. (2008). Peak Daily Water Demand Forecast Modeling Using Artificial Neural Networks. *Journal of Water Resources Planning and Management, 134*(2), 119-128. doi:10.1061//ASCE/0733-9496/2008/134:2/119.

Arandia, E., Ba, A., Eck, B., & McKenna, S. (2016). Tailoring Seasonal Time Series Models to Forecast Short-Term Water Demand. *Journal of Water Resources Planning and Management, 142*(3), 04015067. doi:10.1061/(asce)wr.1943-5452.0000591.

Bai, Y., Li, C., & Xie, J. (2015). Dynamic Forecast of Daily Urban Water Consumption Using a Variable-Structure Support Vector Regression Model. *Journal of Water Resources Planning and Management, 141*(3). doi:0.1061/(ASCE)WR.1943-5452.000045710.1061/(ASCE).

Bakker, M., Vreeburg, J. H. G., van Schagen, K. M., & Rietveld, L. C. (2013). A fully adaptive forecasting model for short-term drinking water demand. *Environmental Modelling Software, 48*(5), 141-151.

Bhanja, S. N. , Mukherjee, A. , Saha, D. , Velicogna, I. , & Famiglietti, J. S. . (2016). Validation of grace based groundwater storage anomaly using in-situ groundwater level measurements in india. *Journal of Hydrology*, *543*, 729-738.

Billings, R. B., & Jones, C. V. (2008). *Forecasting Urban Water Demand* (2nd ed.). Denvor, CO: American Water Works Association.

Bougadis, J., Adamowski, K., & Diduch, R. (2005). Short-term municipal water demand forecasting. *Hydrological Processes, 19*(1), 137-148. doi:10.1002/hyp.5763.

Breiman, L. (2001). Random forests. *Machine Learning, 45*, 5-23.

Chang, C. C., & Lin, C. J. (2001). *Libsvm: a library for support vector machines*.

Chen, G., & Boccelli, D. L. (2018). Forecasting Hourly Water Demands With Seasonal Autoregressive Models for Real-Time Application. *Water Resources Research, 54*(2), 879-894.

Chen, G., Long, T., Xiong, J., & Bai, Y. (2017). Multiple Random Forests Modelling for Urban Water Consumption Forecasting. *Water Resources Management, 31*(15), 4715-4729.

Cherkassky, V., & Ma, Y. (2004). Practical selection of SVM parameters and noise estimation for SVM regression. *Neural Networks, 17*(1), 113-126.

Chollet, F. (2015). Keras. Retrieved from https://github.com/fchollet/keras.

Creaco, E., Pezzinga, G., and Savic, D. (2017). "On the choice of the demand and hydraulic modeling approach to WDN real-time simulation." *Water Resources Research*, 53(7), 6159-6177.

Donkor, E. A., Mazzuchi, T. A., Soyer, R., & Roberson, J. A. (2014). Urban Water Demand Forecasting- Review of Methods and Models. *Journal of Water Resources Planning and Management, 140*(2), 146-156. doi:0.1061/(ASCE)WR.1943-5452.

Gers, F. A. (2001). *Long Short-Term Memory in Recurrent Neural Networks.* (Doctor),

University of Hannover.

Gers, F. A., Schmidhuber, J., & Cummins, F. (2000). Learning to forget: continual prediction with LSTM. *Neural Computation, 12*, 2451-2471.

Ghalehkhondabi, I., Ardjmand, E., Young, W. A., 2nd, & Weckman, G. R. (2017). Water demand forecasting: review of soft computing methods. *Environ Monit Assess, 189*(7), 313. doi:10.1007/s10661-017-6030-3.

Ghiassi, M., Zimbra, D. K., & Saidane, H. (2008). Urban Water Demand Forecasting with a Dynamic Artificial Neural Network Model. *Journal of Water Resources Planning and Management, 134*(2), 138-146. doi:10.1061/(asce)0733-9496(2008)134:2(138).

Guan, H., Li, J., Chapman, M., Deng, F., Ji, Z., & Yang, X. (2013). Integration of orthoimagery and lidar data for object-based urban thematic mapping using random forests. *International Journal of Remote Sensing, 34*(14), 5166-5186.

Guo, G., Liu, S., Wu, Y., Li, J., Zhou, R., & Zhu, X. (2018). Short-Term Water Demand Forecast Based on Deep Learning Method. *Journal of Water Resources Planning and Management, 144*(12), 04018076. doi:10.1061/(asce)wr.1943-5452.0000992.

Hao, Y., Wu, J., Sun, Q., Zhu, Y., Liu, Y., Li, Z., & Yeh, T. J. (2013). Simulating effect of anthropogenic activities and climate variation on Liulin Springs discharge depletion by using the ARIMAX model. *Hydrological Processes, 27*, 2605-2613.

Howe, C. W., & Linaweaver, F. P. (1967). The Impact Price on Residential Water Demand and Its Relation to System Design and Price Structure. *Water Resources Research, 3*(1), 13-32.

Hyndman, R. J., & Khandakar, Y. (2008). Automatic Time Series Forecasting: The forecast Package for R. *Journal of Statistical Software, 26*(3).

Jain, A., Varshney, A., & Joshi, U. (2001). Short-term water demand forecast modelling at IIT Kanpur using artificial neural networks. *Water Resources Management, 15*(5), 299-321.

Kwiatkowski, D., Philips, P. C. B., Schmidt, P., & Shin, Y. (1992). Testing the null hypothesis of stationarity against the alternative of a unit root. *Journal of*

Econometrics, 54, 159-178.

Levin, E., Maddaus, W., Sandkulla, N., & Pohl, H. (2006). Forecasting wholesale demand and conservation savings. *Journal of American Water Works Association, 98*(2), 102-111.

Mikolov, T., Karafiat, M., Burget, L., Cernocký, J., & Khudanpur, S. (2010). *Recurrent neural network based language model*. In: Proceedings of the 11th Annual Conference of the International Speech Communication Association, Makuhari, Chiba, Japan, pp. 1045–1048.

Pacchin, E., Gagliardi, F., Alvisi, S., & Franchini, M. (2019). A Comparison of Short-Term Water Demand Forecasting Models. *Water Resources Management, 33*(4), 1481-1497. doi:10.1007/s11269-019-02213-y

Prosdocimi, I., Kjeldsen, T. R., & Svensson, C. (2013). Non-stationarity in annual and seasonal series of peak flow and precipitation in the UK. *Natural Hazards and Earth System Sciences, 1*(5), 5499-5544.

Qi, Z., Zheng, F., Guo, D., Zhang, T., Shao, Y., Yu, T. Maier, H. R. (2018). A comprehensive framwork to evaluate hydraulic and water quality impacts of pipe breaks on water distribution systems. *Water Resources Research, 54*(10), 8174-8195.

Rasouli, K., Hsieh, W. W., & Cannon, A. J. (2011). Daily streamflow forecasting by machine learning methods with weatherand climate inputs. *Journal of Hydrology, 414-415*, 284-293.

Romano, M., & Kapelan, Z. (2014). Adaptive water demand forecasting for near real-time management of smart water distribution systems. *Environmental Modelling Software, 60*(7), 265-276.

Sardinha-Lourenço, A., Andrade-Campos, A., Antunes, A., & Oliveira, M. S. (2018). Increased performance in the short-term water demand forecasting through the use of a parallel adaptive weighting strategy. *Journal of Hydrology, 558*, 392-404. doi:10.1016/j.jhydrol.2018.01.047

Sundermeyer, M., Schluter, R., & Ney, H. (2012). *LSTM neural networks for language*

555 *modeling*. In: Proceedings of the 12th Annual Conference of the International Speech
556 Communication Association, Portland, Oregon, USA, pp. 601–608.

557 Sutskever, I., Vinyals, O., & Le, Q. V. (2014). *Sequence to sequence learning with neural*
558 *networks*. In: Proceedings of the 28th Conference on Neural Information Processing
559 Systems, Montreal, Canada, pp. 3104–3112.

560 Vapnik, V. (1995). *The nature of statistical learning theory*. New York: Springer.

561 Villarin, M. C., & Rodriguez-Galiano, V. F. (2019). Machine Learning for Modeling Water
562 Demand. *Journal of Water Resources Planning and Management, 145*(5).
563 doi:0.1061/(ASCE)WR.1943-5452.0001067

564 Were, K., Bui, D. T., Dick, O. B., & Singh, B. R. (2015). A comparative assessment of
565 support vector regression, artificial neural networks, and random forests for predicting
566 and mapping soil organic carbon stocks across an Afromontane landscape. *Ecological*
567 *Indicators, 52*, 394-403.

568 Williams, B. M. (2001). Multivariate vehicular traffic flow prediction: evaluation of
569 ARIMAX modeling. *Transportation Research Record Journal, 1776*(1), 194-200.

570 Wong, J. S., Zhang, Q., & Chen, G. (2010). Statistical modeling of daily urban water
571 consumption in Hong Kong- Trend, changing patterns, and forecast. *Water Resources*
572 *Research, 46*. doi:0.1029/2009WR008147

573 Zhang, D., Lindholm, G., & Ratnaweera, H (2018). Use long short-term memory to enhance
574 Internet of Things for combined sewer overflow monitoring. Journal of Hydrology,
575 556, 409-418.

576 Zhang, J., Zhu, Y., Zhang, X., Ye, M., & Yang, J. (2018). Developing a Long Short-Term
577 Memory (LSTM) based model for predicting water table depth in agricultural areas.
578 *Journal of Hydrology, 561*, 918-929.

579 Zheng, F., Zecchin, A., Maier, H., and Simpson, A. (2016). "Comparison of the Searching
580 Behavior of NSGA-II, SAMODE, and Borg MOEAs Applied to Water Distribution
581 System Design Problems." *Journal of Water Resources Planning and Management*,
582 142(7), 04016017.

583 Zheng, F., Zecchin, A., Newman, J., Maier, H., and Dandy, G. (2017). "An Adaptive
584 Convergence-Trajectory Controlled Ant Colony Optimization Algorithm with
585 Application to Water Distribution System Design Problems." *IEEE Transactions on*
586 *Evolutionary Computation*, 21(5), 773-791.

587 Zhou, S. L., McMahon, T. A., Walton, A., & Lewis, J. (2002). Forecasting operational
588 demand for an urban water supply zone. *Journal of Hydrology, 259*, 189-202.

589

590 **Table 1 Inputs of the four models**

Mode types	Time resolutions	Inputs and outputs
LSTM	t=15-minute	$Q_t^0 = f(Q_{t-3}^0, Q_{t-2}^0, Q_{t-1}^0, Q_{t-2}^{-1}, Q_{t-1}^{-1}, Q_t^{-1}, Q_{t+1}^{-1}, Q_{t+2}^{-1}, Q_{t-2}^{-2}, Q_{t-1}^{-2}, Q_t^{-2}, Q_{t+1}^{-2}, Q_{t+2}^{-2})$
	t=1-hour	$Q_t^0 = f(Q_{t-3}^0, Q_{t-2}^0, Q_{t-1}^0, Q_{t-1}^{-1}, Q_t^{-1}, Q_{t+1}^{-1}, Q_{t-1}^{-2}, Q_t^{-2}, Q_{t+1}^{-2})$
	t=24-hour	$Q_t^0 = f(Q_t^{-1}, Q_t^{-2}, Q_t^{-3})$
ARIMA	t=15-minute	$Q_t = f(Q_{t-1}, Q_{t-2}, \ldots, Q_{t-671}, Q_{t-672})$
	t=1-hour	$Q_t = f(Q_{t-1}, Q_{t-2}, \ldots, Q_{t-671}, Q_{t-672})$
	t=24-hour	$Q_t = f(Q_{t-1}, Q_{t-2}, \ldots, Q_{t-55}, Q_{t-56})$
SVR	t=15-minute	$Q_t^0 = f(Q_{t-3}^0, Q_{t-2}^0, Q_{t-1}^0, Q_{t-2}^{-1}, Q_{t-1}^{-1}, Q_t^{-1}, Q_{t+1}^{-1}, Q_{t+2}^{-1}, Q_{t-2}^{-2}, Q_{t-1}^{-2}, Q_t^{-2}, Q_{t+1}^{-2}, Q_{t+2}^{-2})$
	t=1-hour	$Q_t^0 = f(Q_{t-5}^0, Q_{t-4}^0, Q_{t-3}^0, Q_{t-2}^0, Q_{t-1}^0, Q_t^{-1}, Q_t^{-2})$
	t=24-hour	$Q_t^0 = f(Q_t^{-1}, Q_t^{-2}, Q_t^{-3}, Q_t^{-4}, Q_t^{-5})$
RF	t=15-minute	$Q_t^0 = f(Q_{t-5}^0, Q_{t-4}^0, Q_{t-3}^0, Q_{t-2}^0, Q_{t-1}^0, Q_t^{-1}, Q_t^{-2})$
	t=1-hour	$Q_t^0 = f(Q_{t-5}^0, Q_{t-4}^0, Q_{t-3}^0, Q_{t-2}^0, Q_{t-1}^0, Q_t^{-1}, Q_t^{-2})$
	t=24-hour	$Q_t^0 = f(Q_t^{-1}, Q_t^{-2}, Q_t^{-3})$

591

592

593 **Table 2 Statistics of the model prediction errors for the total water demands**

Time resolutions	Models	*MAPE*	*NSE*	R^2	*RMSE* (m^3)
15-minute	***LSTM***	***1.40%***	***0.991***	***0.991***	***315***
	ARIMA	2.14%	0.974	0.975	551
	SVR	2.01%	0.985	0.986	421
	RF	2.03%	0.984	0.984	425
1-Hour	***LSTM***	***2.56%***	***0.978***	***0.981***	***1976***
	ARIMA	4.26%	0.937	0.937	3367
	SVR	3.40%	0.963	0.966	2587
	RF	3.70%	0.945	0.945	3153
24-Hour	***LSTM***	***2.89%***	***0.820***	***0.822***	***55,605***
	ARIMA	2.94%	0.811	0.821	55,463
	SVR	3.82%	0.680	0.769	74,181
	RF	3.08%	0.816	0.821	56,179

594

595

596 **Table 3 Statistics of prediction errors for models used for multiple successive**

597 **data forecasts**

No. of successive predictions (k)	Models	*MAPE*	*NSE*	R^2	*RMSE* (m^3)
k=4	**LSTM**	**2.21%**	**0.980**	**0.981**	**475**
	ARIMA	3.19%	0.954	0.954	728
	SVR	3.05%	0.970	0.973	591
	RF	3.11%	0.959	0.959	685
k=96	**LSTM**	**5.23%**	0.899	0.909	1075
	ARIMA	16.28%	0.206	0.348	3018
	SVR	7.41%	0.832	0.836	1390
	RF	8.19%	0.751	0.754	1692

598

599

600 **Table 4 Statistics of model prediction errors for data with abrupt changes**

Time resolutions	Models	*MAPE*	*NSE*	R^2	*RMSE* (m^3)
15-minute	**LSTM**	**2.96%**	**0.961**	**0.962**	**596**
	ARIMA	5.58%	0.897	0.909	967
	SVR	4.56%	0.939	0.940	744
	RF	5.49%	0.916	0.916	873
1-Hour	**LSTM**	**2.89%**	**0.979**	**0.982**	**2111**
	ARIMA	5.75%	0.913	0.983	4307
	SVR	4.94%	0.956	0.974	3057
	RF	6.95%	0.884	0.973	4973
k=4*	**LSTM**	**3.56%**	**0.962**	**0.963**	**588**
	ARIMA	5.33%	0.929	0.936	803
	SVR	4.69%	0.933	0.938	780
	RF	4.76%	0.920	0.923	853
k=96*	**LSTM**	7.19%	0.821	0.862	1274
	ARIMA	15.69%	0.315	0.368	2492
	SVR	9.57%	0.688	0.731	1681
	RF	9.36%	0.678	0.732	1708

601 **k*=4 and 96 represents 4 and 96 successive predictions with 15-min resolution.

602

603 **Table 5 Statistics of prediction errors for models used for data with a relatively**
604 **uncertainty level**

Time resolutions	Models	*MAPE*	*NSE*	R^2	*RMSE* (m^3)
15-minute	**LSTM**	**11.77%**	**0.924**	**0.935**	**0.74**
	ARIMA	19.94%	0.843	0.843	0.94
	SVR	17.78%	0.856	0.861	0.90
	RF	18.95%	0.856	0.856	0.90
1-hour	**LSTM**	**10.29%**	**0.942**	**0.942**	**2.18**
	ARIMA	19.14 %	0.860	0.859	3.39
	SVR	14.59 %	0.898	0.905	2.92
	RF	13.90%	0.899	0.900	2.86
24-hour	**LSTM**	**1.36%**	**0.878**	**0.895**	**11.23**
	ARIMA	1.86%	0.811	0.852	13.99
	SVR	7.66%	-1.704	0.280	52.92
	RF	2.64%	0.425	0.642	24.39

605

606

607

608 **Figure 1: The structure of a long-short term memory (LSTM) network, where**
609 **the dotted lines represent the recurrent procedure**

610

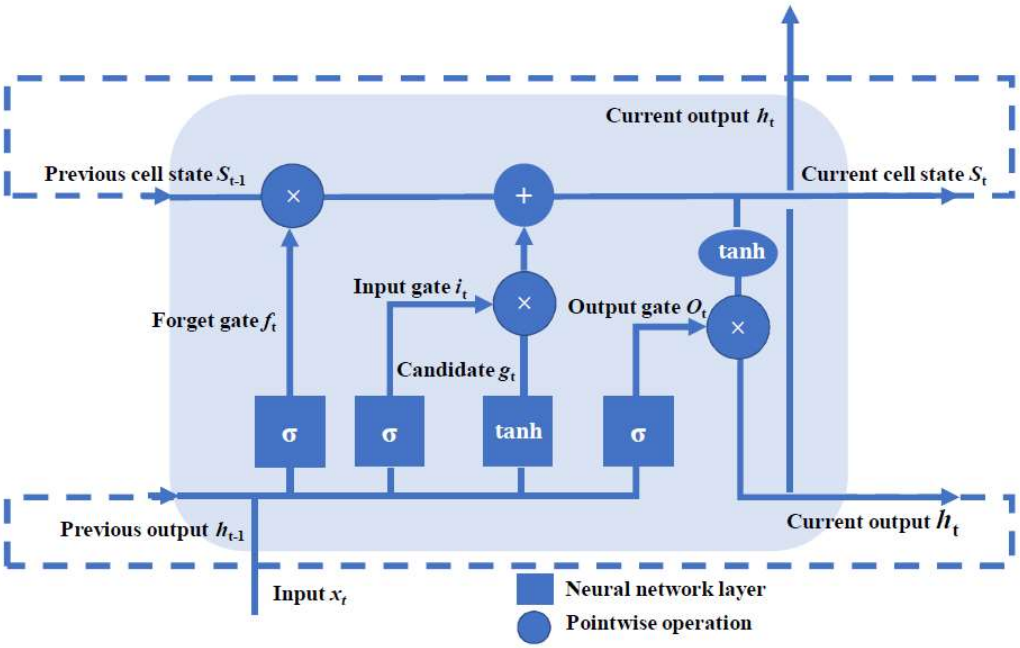

611

612 **Figure 2: Water treatment plants (WTPs) distributed in the city of Hefei, China,**
613 **with green liens representing the water distribution pipelines.**

614

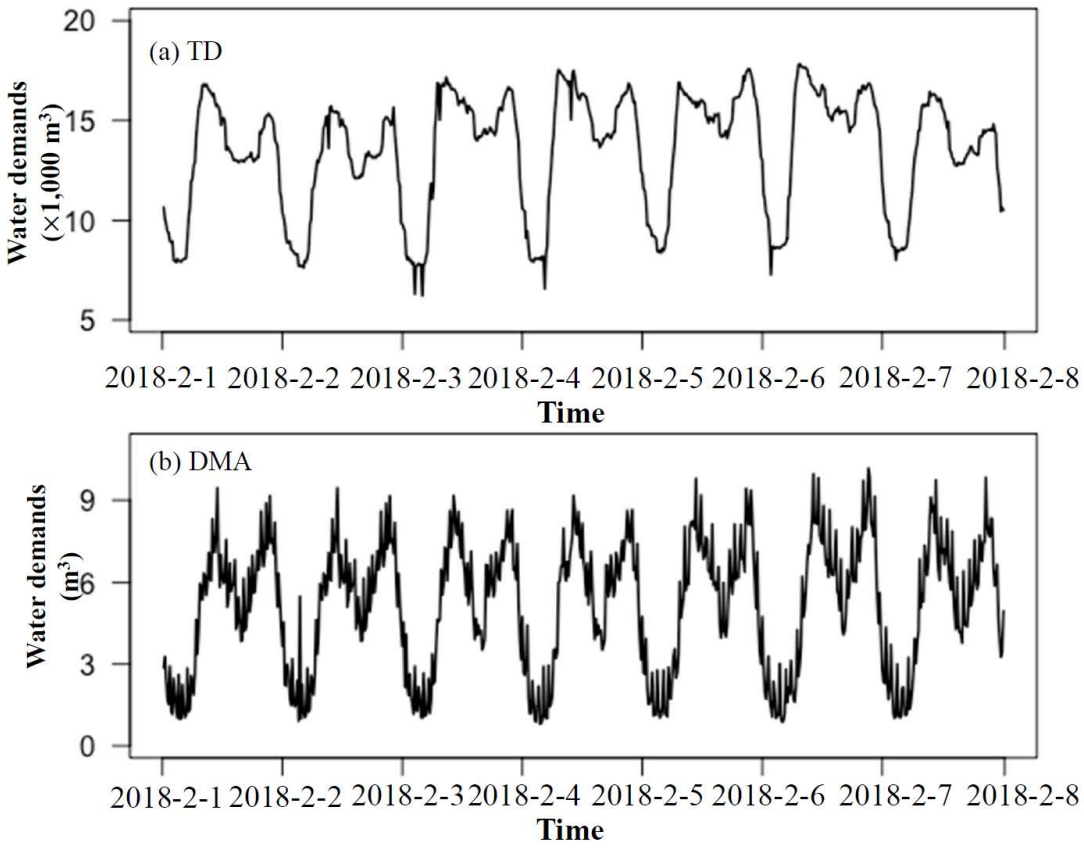

615

616 **Figure 3: Records of total water demands (TD) and from a DMA with 15-min**

617 **resolution**

618

619

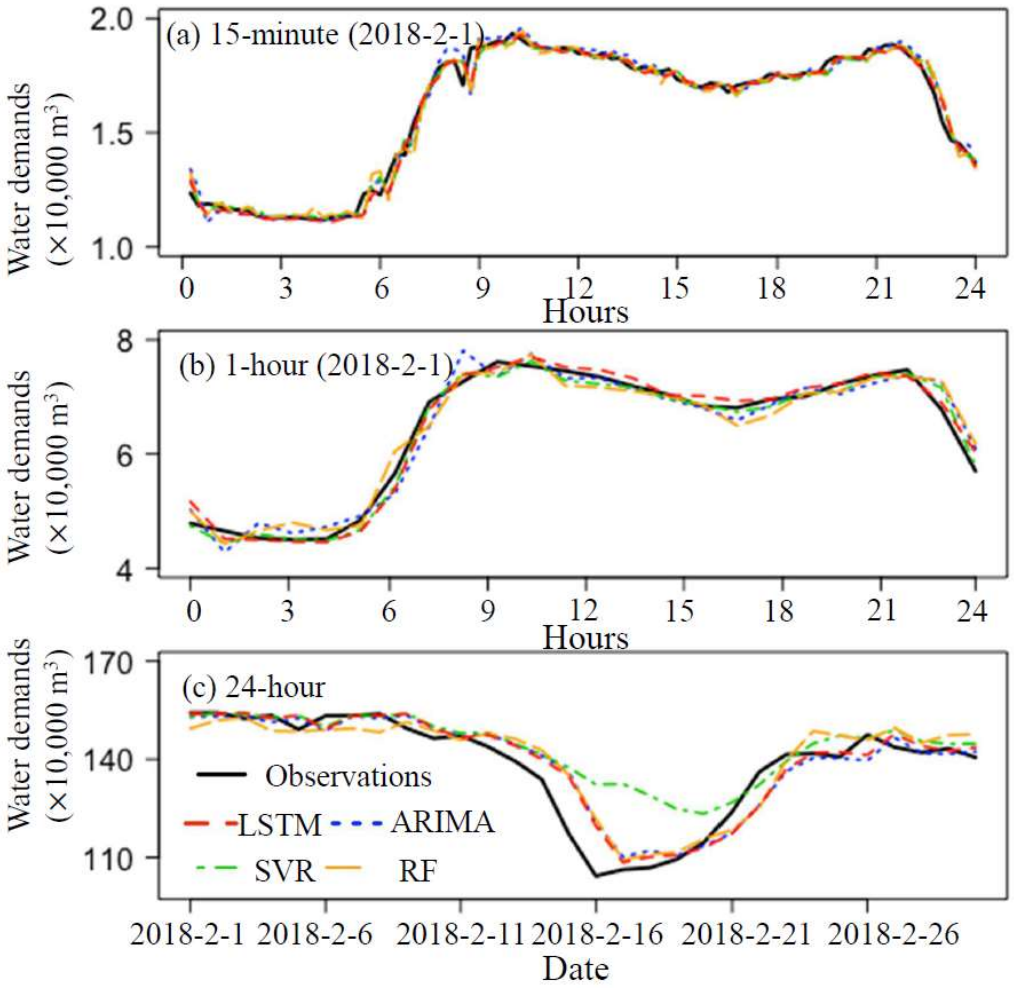

Figure 4: Predictions versus observations for the four models applied to the total water demands (TD)

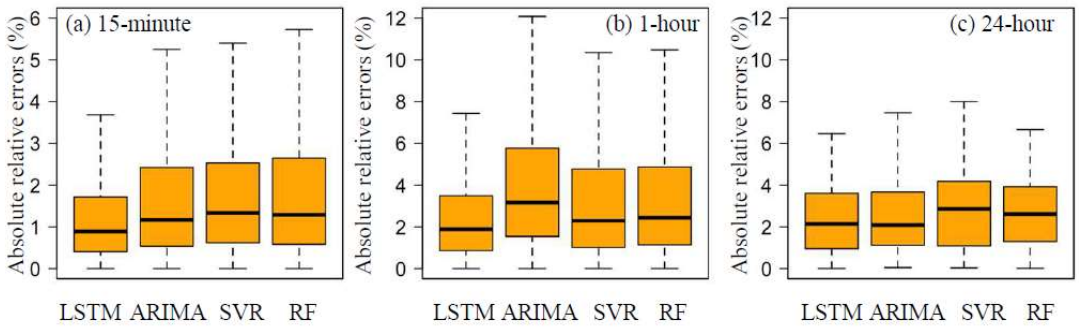

Figure 5: Absolute relative errors of the model predictions for the total water demands

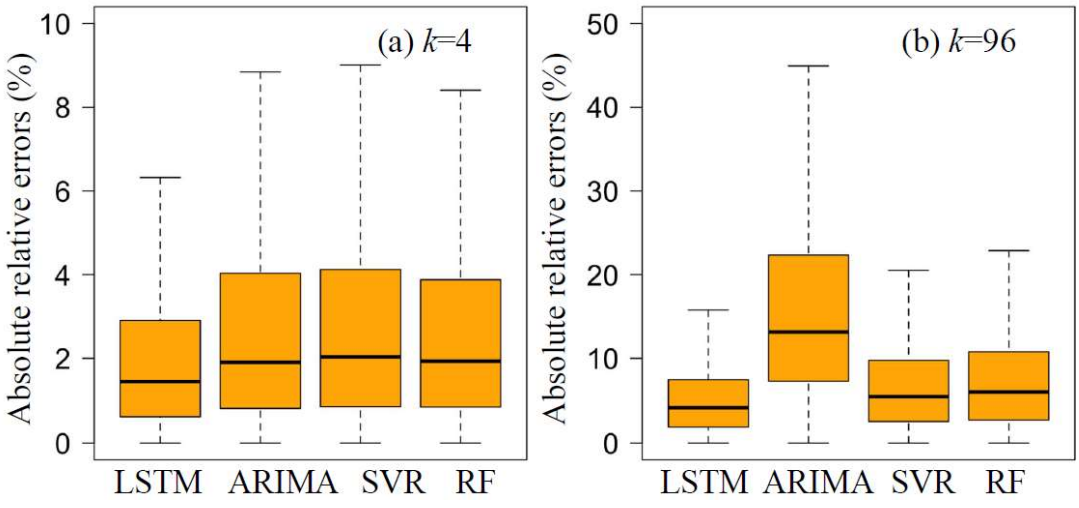

Figure 6: Absolute relative errors for models used to predict multiple successive data points, where *k* is the number of multiple successive data points

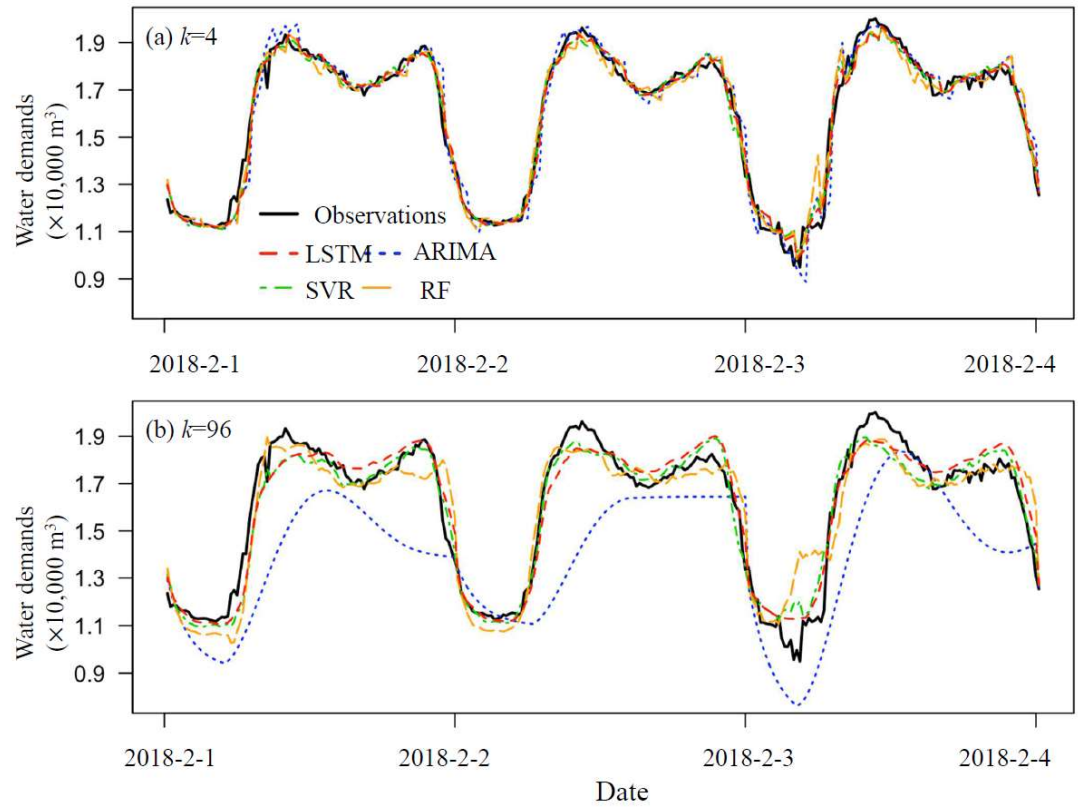

Figure 7: Predictions versus observations for the four models used to generate multiple successive data points

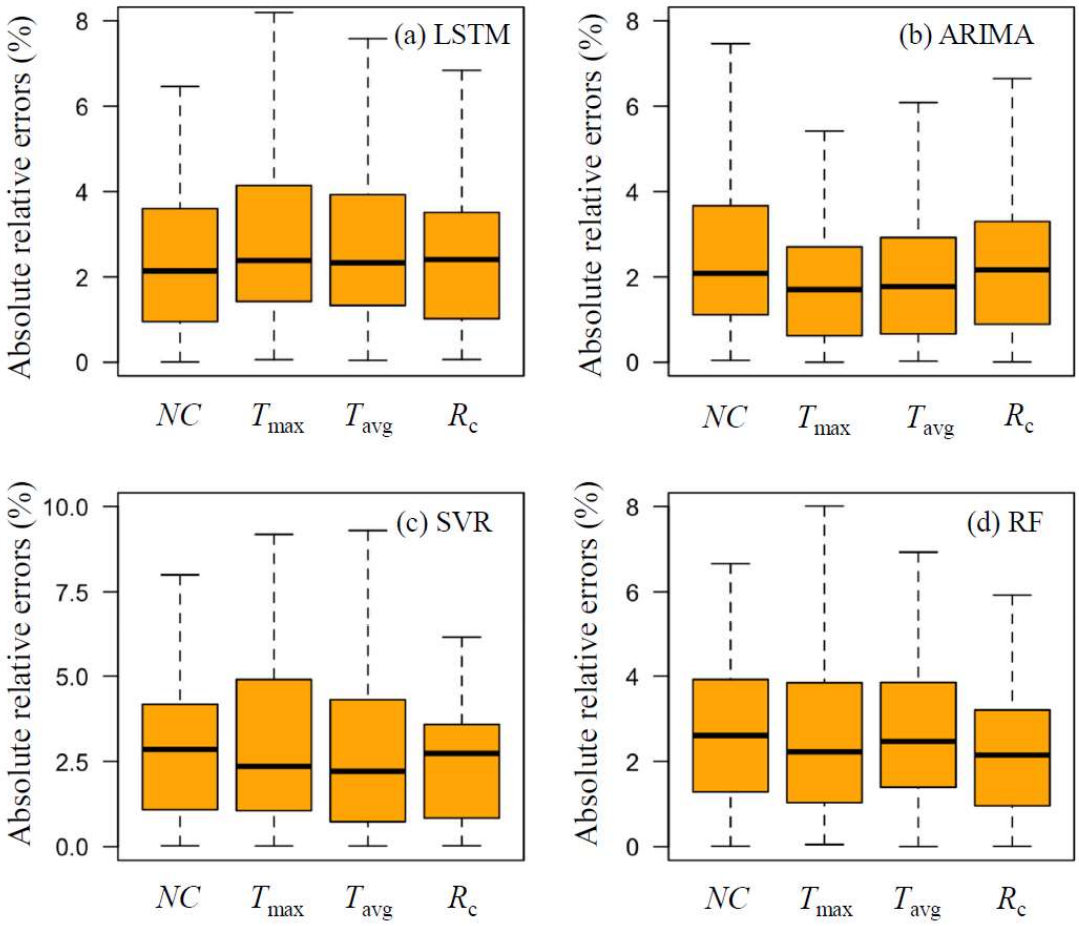

Figure 8: Absolute relative errors of the four models with different external parameters applied to the total water demands with the 24-hour resolution